

# Simultaneous optimization of distribution and gain of piezoelectric sensor networks for the improvement of active vibration control

Augusto H. Shigueoka and Marcelo A. Trindade

Department of Mechanical Engineering, São Carlos School of Engineering, University of São Paulo, Av.  
Trabalhador São-Carlense, 400, São Carlos-SP, 13566-590, Brazil

## Abstract

Modal sensors and actuators working in closed loop enable to observe and control independently specific vibration modes, reducing the apparent dynamical complexity of the system and the necessary energy to control them. Modal sensors may be obtained by a properly designed weighted sum of the output signals of an array of sensors distributed on the host structure. Although several research groups have been interested on techniques for designing and implementing modal filters based on a given array of sensors, the effect of the array topology on the effectiveness of the modal filter has received much less attention. In particular, it is known that some parameters, such as size, shape and location of a sensor, are very important. This work presents the optimization of the distribution of a network of piezoelectric sensors bonded to a clamped plate. A piezoelectric actuator is considered for the excitation of the plate and it is desired to design discrete modal filters able to isolate the response of selected vibration modes.

## 1. INTRODUCTION

The use of piezoelectric materials (specially piezoceramics) as sensing and actuating elements has been extensively studied due to the possibility of building them as lightweight and compact devices in several geometric configurations, since they are relatively inexpensive and present the necessary electromechanical coupling [1]. In the last decades, a great research effort has been put on the modeling of the electromechanical coupling of structures with piezoelectric elements (actuators/sensors). In terms of applications, integrated piezoelectric sensors and actuators have been most often applied to the active control of mechanical vibration and noise in structures subjected to several types of excitation, or even self-excited structures, especially for aeronautic and aerospace applications [1].

On the other hand, the performance of integrated systems applied to active vibration and noise control can be substantially improved by the use of high quality modal filters [2, 3, 4]. In this context, the development of active control strategies with optimal performance using modal sensors and actuators has been the object of intensive research. Modal sensors and actuators working in closed loop enable to observe and control independently specific vibration modes, reducing the apparent dynamical complexity of the system and the necessary energy to control them [5, 6, 7]. The high performance of modal controllers depends on several parameters. The size, form and effective electromechanical coupling coefficient of a piezoelectric material must be considered to the development of modal sensors and actuators. Although pioneer works have proposed continuous modal sensors and actuators [8], the evolution of modal filter techniques and its applications to active vibration control indicates several advantages in the use of an array of discrete sensors instead [9].

Continuous modal sensors are designed to ensure shape coupling between sensing material and elastic strain due to the target vibration modes of the host structure [7, 8]. An array of sensors, on the other

hand, is in general composed by small piezoceramic patches and depends on a convenient weighted sum of the sensors signals to achieve an output signal with the properties of a high-performance modal filter [5, 6]. Recent works apply modal filters using an array of discrete sensors for the construction of smart integrated systems with built-in damage detection capabilities [10, 11]. Several methodologies have been used for the evaluation of the weighting coefficients for the output signals measured by an array of sensors. They can be divided in three groups: target modes output match, optimization techniques and frequency response function (FRF) matrix inversion. Whenever the target mode shapes are known/predicted and their reading in terms of output amplitude in each sensor of the array can be identified, a technique, proposed by Meirovitch and Baruh [12] and based on the orthogonality of normal modes, considers that the weighting coefficients should match the output of each sensor for the target mode. This technique may be strongly affected by spatial aliasing. The weighting coefficients may also be evaluated using an optimization algorithm to minimize the difference between the weighted response and a desired modal response. Shelley [9] proposed an on-line adaptation algorithm to estimate the desired modal response and update the weighting coefficients. The third group of methods is based on the inversion of the FRF matrix, which can be either predicted by a numerical model [2] or experimentally measured [9, 13], in order to shape the target filtered response.

These techniques may lead to high-performance modal filters, but generally within a limited frequency range [6]. Preumont et al. [6] have suggested that the frequency range of high-performance filtering depends on the relation between the number of vibration modes to be filtered, in that frequency range, and the number of sensors in the array. They concluded that the number of sensors in the array should be larger than the number of vibration modes to be filtered. Although this is true for an arbitrarily distributed array of sensors, it is possible to show that the location of the sensors, that is the array topology, have a significant effect on the observability of the vibration modes and, thus, on the filtering performance of modal filters derived from it. Therefore, it should be possible to optimize the array topology and, consequently, increase the number of filtered vibration modes, thus the frequency range, for a given number of sensors available.

Discrete spatial modal filters were already used for quasi-modal or semi-modal feedback and feedforward noise and vibration control [3, 13, 14]. The theory developed by Meirovitch and Baruh [12] shows that perfect modal sensors combined to perfect modal actuators should allow to control independently a given set of vibration modes. They named their feedback control law as Independent Modal Space Control (IMSC). However, it is not feasible in practice since there are no perfect modal sensors and actuators. Therefore, some effect on non-targeted vibration modes should be expected due to residual filtering errors of sensors and/or actuators. Nevertheless, realistic modal sensors and/or actuators should at least be able to improve feedback control roll-off performance. A modification of IMSC was successfully implemented by Baz and Poh [14] using only one actuator and three sensors aiming at controlling the first two vibration modes.

Topology optimization techniques are common in advanced structural design, for instance the simultaneous design of actuated mechanical devices, and often present a multiobjective character [15, 16, 17]. Techniques for topology optimization include but are not limited to genetic algorithm search methods. Genetic algorithm (GA) methods are search algorithms based on the survival of the fittest theory applied for a structured set of parameters [18]. GA-based optimization methods have also been used for the design optimization of controlled structures. Unlike conventional optimization techniques, GA-based ones do not require continuity or differentiability of the objective function with respect to design variables. Besides, they evaluate simultaneously a population of individuals (sets of parameters) and, hence, the probability of converging to a non-global optimum is reduced. Another advantage of GA-based optimization techniques is the possibility of considering both float and binary design parameters, allowing for instance to account for different design configurations (topologies) in addition to material and geometrical parameters.

This work extends previous ones in which modal filters based on optimally located arrays of piezoelectric sensors applied to a free-free rectangular plate were designed and experimentally validated with satisfactory results [19, 20, 21]. Differently from the previous works, in the present one, the mobility FRF

is considered as target function for the evaluation of weighting coefficients, a larger number of options are considered for the distribution of the piezoelectric sensors on a clamped plate and a piezoelectric actuator is considered as excitation for the optimization of the resulting modal filter.

## 2. DESIGN OF MODAL FILTERS

The design of a modal filter from an array of sensors requires the output signals of each sensor to be weighted and summed such that the responses of target vibration modes are maximized relative to those of undesired vibration modes. Therefore, it is possible to consider the mobility FRF of an equivalent single degree of freedom system with natural frequency  $\omega_i$  and damping factor  $\zeta_i$ , corresponding to the target  $i$ -th vibration mode, as the desired FRF of the modal filter output, which can be written as

$$g_i(\omega) = \frac{2j\zeta_i\omega_i\omega}{\omega_i^2 - \omega^2 + 2j\zeta_i\omega_i\omega}. \quad (1)$$

Whenever the vibration modes are weakly damped and relatively well spaced, the resonance peaks are well defined and, thus, (1) represents a realistic objective for the filtered FRF signal. Let  $\mathbf{Y}$  be a matrix with columns that represent the FRFs of the  $n$  selected sensors in the array and discretized in a frequency domain  $[\omega_1, \dots, \omega_m]$ . Let  $\mathbf{G}_i = [g_i(\omega_1), \dots, g_i(\omega_m)]$  be the vector representing (1) in the discrete frequency domain. The vector of coefficients  $\alpha_i$  which equates the filtered output (weighted sum of sensors outputs) to the one defined by  $\mathbf{G}_i$  is the solution of

$$\begin{bmatrix} Y_1(\omega_1) & \cdots & Y_n(\omega_1) \\ \vdots & \ddots & \vdots \\ Y_1(\omega_m) & \cdots & Y_n(\omega_m) \end{bmatrix} \begin{bmatrix} \alpha_{i1} \\ \vdots \\ \alpha_{in} \end{bmatrix} = \begin{bmatrix} g_i(\omega_1) \\ \vdots \\ g_i(\omega_m) \end{bmatrix}. \quad (2)$$

In general, the linear system defined by (2) admits only approximate solutions, which will be denoted  $\alpha_i^\dagger$ . The vector of weighting coefficients  $\alpha_i^\dagger$  represents the best solution, in a least squares sense, for the design of a modal filter which isolates the  $i$ -th vibration mode response. If several vibration modes are to be considered simultaneously as target modes for the filter design, it is necessary to define  $\mathbf{G}$  as the matrix of target FRFs with dimension  $m \times p$ , where  $p$  denotes the number of target modes. Consequently, the approximate solution of (2),  $\alpha^\dagger$ , is a matrix of dimension  $n \times p$ , that is one column vector of weighting coefficients for each one of the target modes. This may be written in a compact form as

$$\mathbf{Y}\alpha^\dagger = \mathbf{G}. \quad (3)$$

Actually,  $\mathbf{Y}\alpha^\dagger$  approximates  $\mathbf{G}^\dagger$ , a matrix with columns that are the orthogonal projection of the columns of  $\mathbf{G}$  onto the space spanned by the columns of  $\mathbf{Y}$ . The traditional Moore-Penrose pseudo-inverse solution of (3) for a full column rank  $\mathbf{Y}$  matrix (with columns that are linearly independent) may be obtained by pre-multiplying (3) by  $\mathbf{Y}^H$ ,

$$\mathbf{Y}^H\mathbf{Y}\alpha^\dagger = \mathbf{Y}^H\mathbf{G}, \text{ such that } \alpha^\dagger = (\mathbf{Y}^H\mathbf{Y})^{-1}\mathbf{Y}^H\mathbf{G}. \quad (4)$$

On the other hand, for a full column rank matrix, the inversion of  $\mathbf{Y}^H\mathbf{Y}$  is unnecessary and computationally inefficient, since  $\mathbf{Y}$  may be decomposed through QR decomposition, where  $\mathbf{Q}$  is an orthonormal matrix and  $\mathbf{R}$  is upper triangular, such that  $\mathbf{Y} = \mathbf{Q}\mathbf{R}$  and (4) can be rewritten, after expansion and accounting for  $\mathbf{Q}^H\mathbf{Q} = \mathbf{I}$ , as

$$\alpha^\dagger = \mathbf{R}^{-1}\mathbf{Q}^H\mathbf{G}. \quad (5)$$

Notice that evaluating the inverse of  $\mathbf{R}$  is not necessary, instead the upper triangular linear system,  $\mathbf{R}\alpha^\dagger = \mathbf{Q}^H\mathbf{G}$ , is solved through back substitution, which is computationally more efficient. For all the cases studied here, the solution through QR decomposition was always convenient, since the FRF matrix has had full column rank. If at least two columns of the FRF matrix are linearly dependent, the singular

value decomposition (SVD) is the suitable method to approximate the least squares solution. In practice, the truncation of matrix  $\mathbf{Y}$  over a given frequency range will affect its QR decomposition and, thus, the approximate solution of the linear system (3). Recent works have shown that there is a value for truncation frequency such that all vibration modes inside a given frequency range are perfectly filtered, except the target ones, whereas resonances larger than the truncation frequency are not filtered [6].

### 3. APPLICATION TO A PLATE WITH PIEZOELECTRIC SENSORS

In this section, the modal filter design technique presented in the previous section is applied to a plate with bonded piezoceramic patches, acting as sensors, to analyze its effectiveness and evidence its limitations. The host structure considered is a free rectangular aluminum plate, of dimensions  $500 \times 400 \times 2$  mm, and has twelve identical thickness-poled PZT-5H piezoceramic patches bonded to its upper surface. The external excitation is also performed using four identical PZT-5H piezoceramic patches, serving as actuators in this case, bonded to the lower surface of the plate. The four actuators are connected to the same electrode and are placed such that reasonable control authority for the first vibration modes can be obtained. The piezoceramic patches have dimensions  $25 \times 25 \times 0.5$  mm. Figure 1 presents a geometric description of the model. The material properties are: i) Aluminum – Young's modulus 70 GPa, Poisson's ratio 0.33, mass density  $2700 \text{ kg/m}^3$ ; and ii) PZT-5H – mass density  $7500 \text{ kg/m}^3$ , and elastic  $c_{11}^E = c_{22}^E = 127 \text{ GPa}$ ,  $c_{33}^E = 117 \text{ GPa}$ ,  $c_{12}^E = 80.2 \text{ GPa}$ ,  $c_{13}^E = 84.7 \text{ GPa}$ ,  $c_{44}^E = c_{55}^E = 23.0 \text{ GPa}$ ,  $c_{66}^E = 23.5 \text{ GPa}$ , piezoelectric  $d_{31} = d_{32} = -274 \text{ pC/N}$ ,  $d_{33} = 593 \text{ pC/N}$ ,  $d_{15} = d_{24} = 741 \text{ pC/N}$  and dielectric  $\epsilon_{11}^T = \epsilon_{22}^T = 27.7 \text{ nF/m}$ ,  $\epsilon_{33}^T = 30.1 \text{ nF/m}$  constants.

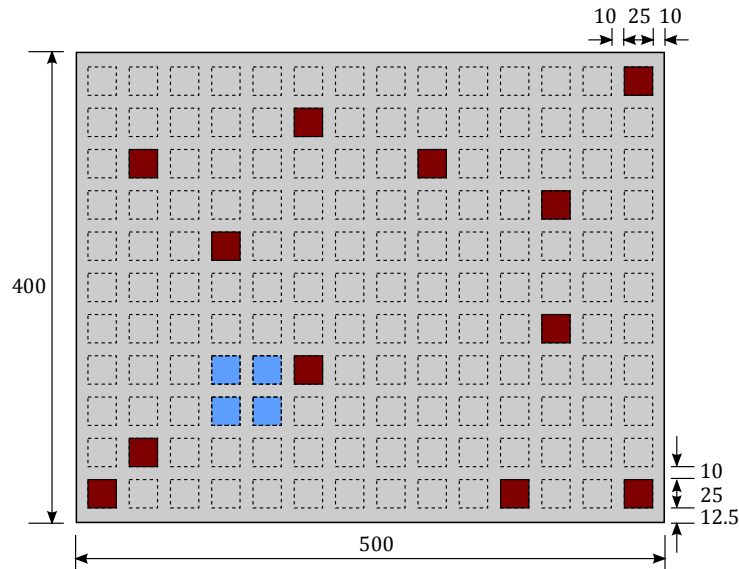


**Figure 1.** Aluminum plate with twelve piezoceramic sensors bonded on the upper surface, placed arbitrarily within the 154 possible locations, and four piezoceramic actuators bonded on the lower surface (dimensions in mm).

A classical sandwich plate finite element model recently developed was used. The three layers are supposed to be made of transversely poled piezoelectric materials. Electrodes fully cover the top and bottom skins of all layers so that only through-thickness electric field and displacement are considered. For simplicity, all layers are assumed to be made of orthotropic piezoelectric materials, perfectly bonded and in plane stress state. Kirchhoff-Love theory is retained for the sandwich beam surface layers, while the core is assumed to behave as a Reissner-Mindlin plate. A four-node rectangular finite element, with 7 mechanical and 3 electrical degrees of freedom (dof) per node, was considered for the discretization of the sandwich plate. The nodal mechanical dof are the four in-plane displacements of the upper and lower surface layers, the transverse displacement and its derivatives with respect to the two in-plane coordinates. The nodal electrical dof are the electric displacements (electric charge surface density) on

each of the three layers. During assembling procedure, equipotential boundary conditions are imposed to piezoelectric patches connected to the same electrode. Through post-processing, the model allows either electric charge or voltage outputs.

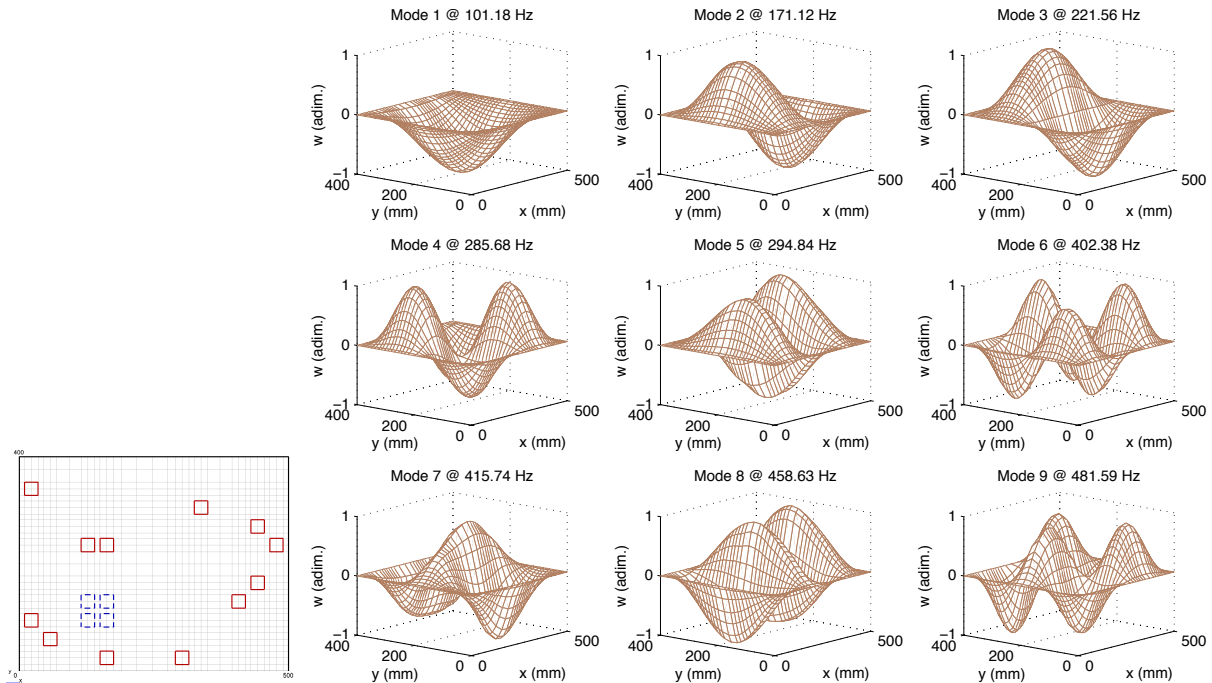


**Figure 2.** Finite element mesh, mode shapes and natural frequencies for the first nine vibration modes of the plate with arbitrarily distributed piezoceramic patches.

**Table 1.** First twenty natural frequencies of the aluminum plate with bonded piezoceramic patches.

Mode	1	2	3	4	5	6	7	8	9	10
Frequency (Hz)	101.2	171.1	221.6	285.7	294.8	402.4	415.7	458.6	481.6	561.6
Mode	11	12	13	14	15	16	17	18	19	20
Frequency (Hz)	589.1	662.6	674.0	735.4	742.0	763.3	837.0	924.7	936.7	982.5

Figure 2 shows the finite element mesh used for the modal analysis of an arbitrary distribution of the piezoelectric sensors. It also shows the first nine vibration modes of the plate with piezoelectric sensors and actuator. The natural frequencies for the first twenty vibration modes, contained within a [0,1000] Hz frequency range, are also shown in Table 1.

The frequency response functions between the applied voltage to the actuator, composed of four piezoceramic patches bonded to the lower surface of the plate and connected to a single electrode, and the voltage induced in the twelve piezoceramic sensors, bonded to the upper surface of the plate and connected to independent circuits, are shown in Figure 3.

#### 4. OPTIMIZATION OF SENSORS' SPATIAL DISTRIBUTION

Previous analyses [19] have shown that although, in average, the number of modes, and thus the frequency range of the modal filter, is limited by the number of sensors considered, properly selected distributions could increase the frequency range, for a given number of sensors, or reduce the number of sensors, for a given frequency range. Therefore, for a given number of sensors in a network, their distribution could be optimized to enhance the performance of the resulting modal filters.

After some numerical simulations with straightforward distributions, it becomes clear that the relation between the sensors' network distribution and the filtering performance is quite complex, even when the mode shapes are known. Hence, optimal solutions require a more advanced strategy. GAs are more

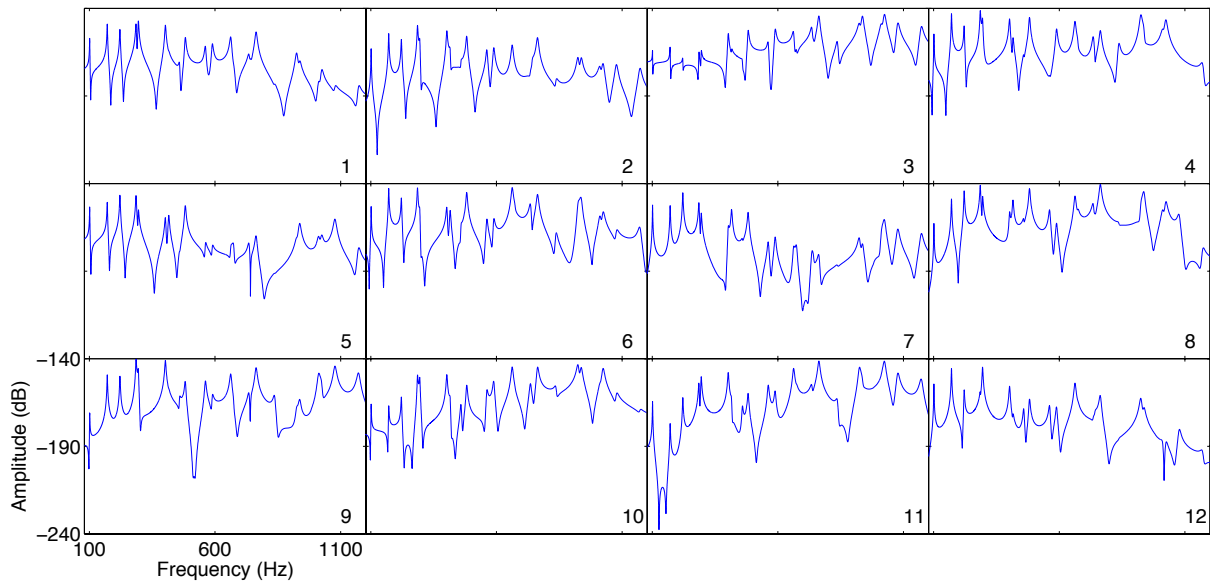


**Figure 3.** Frequency response function between piezoelectric actuator and sensors.

suitable search methods in these cases when the research space is too large, strongly multimodal and non-linear. It is chosen here to setup a GA search by defining a random initial population formed by so-called individuals with chromosomes that are composed of twelve genes as illustrated in Figure 4. Each gene is an integer number from 1 to 36 representing the sensor index. Therefore, one individual represents a topology formed by the twelve sensors defined by its genes. A similar approach for the optimization of sensors positioning was presented in [11, 19].



**Figure 4.** Arbitrary representation of a sensors' network distribution candidate containing 12 sensors.

Following the standard GA evolutive process, the initial population is considered to evolve along a set of generations through reproduction (crossover), mutation and selection operations. While reproduction and mutation operations aim to provide diversity to the population, the selection operation aims to rank individuals with respect to a fitness or objective function. Since this is a random search algorithm, the optimal results are dependent on the initial population and on the reproduction, mutation and selection parameters. However, it is expected that for a sufficiently large number of generations or size of the initial population, the algorithm will converge to the global optimum.

Since any individual of the population is composed by twelve different integer numbers in the domain  $[1, \dots, 154]$ , a specific routine was written to build the initial population. For each individual, the routine scrambles randomly a vector of integers from 1 to 154 and, then, the first 12 elements of the scrambled vector define the corresponding individual. This procedure is repeated for all individuals in the initial population. The selection of the first 12 elements in the scrambled vector does not imply a tendency since the distribution of the sensor indices in the vector is equiprobable.

The mutation operation, considered in this work, consists in replacing one of the 12 genes (sensors), selected randomly, of an individual by another one, selected randomly from the complementary group of sensors, that is, from the 142 remaining sensors not present in the individual. This procedure prevents the generation of an individual with repeated genes. The reproduction (crossover) operation combines the initial and final sections of two individuals (parents) to form a new individual (child), where the breaking position of the parents' sequences (chromosomes) is defined randomly. In this case, the generation of an individual with repeated genes is possible and, when this is the case, the fitness function of this individual is not evaluated to save computational time; instead a small fitness value is attributed to it, such that its selection probability is also small. The selection operation is based on a stochastic universal sampling

algorithm, where the expectation of individuals in the population is evaluated from a fitness ranking.

Besides the choice of reproduction, mutation and selection operators, it is necessary to define the size of the initial population ( $N$ ), the number of best individuals (elite) which are kept unmodified from one generation to another ( $\Sigma$ ), the percentage of the population in each generation which are generated by crossover ( $T_c$ ) and the total number of generations the population evolves ( $N_p$ ). Once defined  $T_c$ , the remaining part of population is generated by either the previous elite or mutation operation. Apart from the procedures proposed for the construction of the initial populations, the mutation operation and the parameters' definition, the optimization was performed using operators and algorithms of MATLAB Genetic Algorithm and Direct Search (GADS) Toolbox.

The objective of the present optimization is to find the topology of an array with twelve sensors that maximizes the filtering quality, over a given frequency range, of modal filters designed to isolate a given set of resonances of the structure. First, four cases were studied using the following as target vibration modes to be isolate by the modal filters:  $\{1\}$ ,  $\{1,2\}$ ,  $\{1,2,3\}$  and  $\{1,2,3,4\}$ . The target frequency range is  $[0, 750]$  Hz, which is higher than the limit frequency  $\omega_l = 600$  Hz for the present case and, as shown in Table 1, contains fifteen resonances (four above  $\omega_l$ ). Therefore, the FRF truncation frequency is defined as  $\omega_t = 750$  Hz such that, for an arbitrary sensors' distribution, no filtering quality can be guaranteed along the frequency range, while an optimal distribution can maximize this quality. For implementation purposes, the objective function to be minimized is then defined as the residual error norm

$$J = \|\mathbf{G}_t - \mathbf{Y}_t \boldsymbol{\alpha}^\dagger\|_2, \quad (6)$$

where  $\mathbf{G}_t$  and  $\mathbf{Y}_t$  are the target and measured, by each sensor, FRFs truncated at frequency  $\omega_t$  and  $\boldsymbol{\alpha}^\dagger$  is the vector of weighting coefficients, evaluated using  $\mathbf{G}_t$  and the QR decomposition of matrix  $\mathbf{Y}_t$  in (5). In the case where more than one target function is considered, the cost function  $J$  is defined as the arithmetic mean of the residual error norm (6) for each individual modal filter (or target function).

Then, the sensors' distribution is optimized in order to provide an effective modal filter aimed at isolating a set of resonances simultaneously. This is done by considering a N-dof frequency response function as target function, constructed from (1), such that

$$g_s(\omega) = \sum_i g_i(\omega). \quad (7)$$

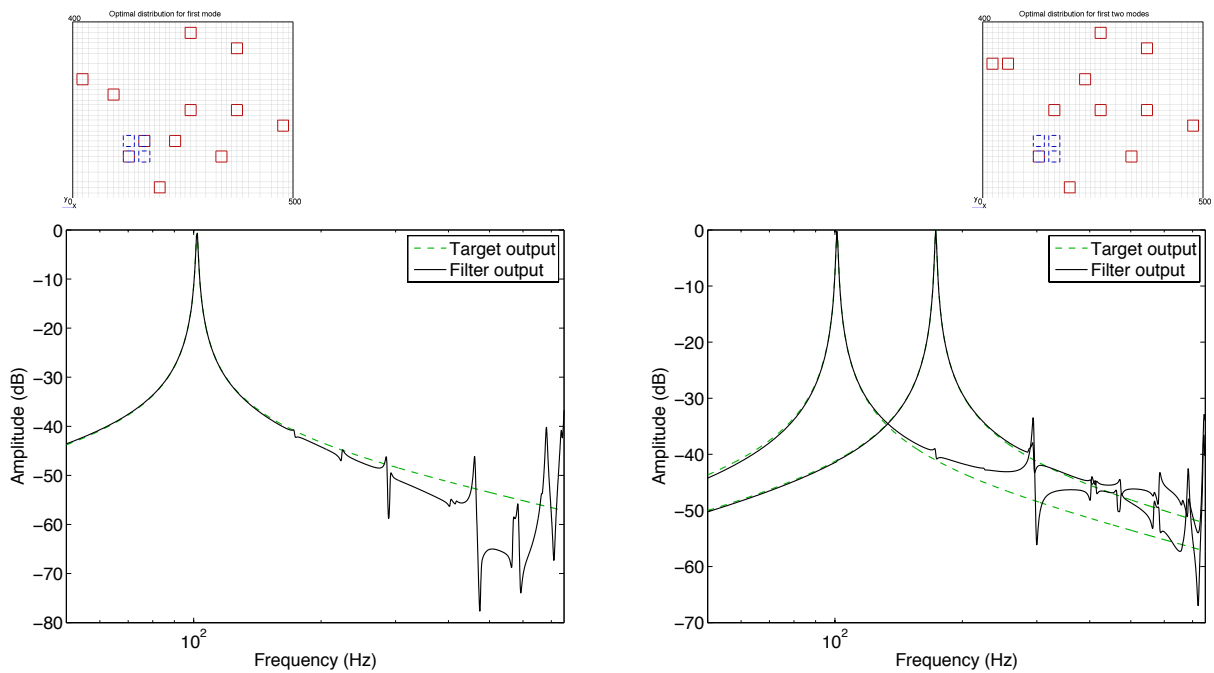
As in the previous case, the N-dof frequency response function is represented by a vector in the discrete frequency domain and is truncated at frequency  $\omega_t$ , leading to  $\mathbf{G}_t$ . This vector is then used in (5) to evaluate the vector of weighting coefficients  $\boldsymbol{\alpha}^\dagger$ . This then leads to three additional cases using N-dof target functions composed of the response of the following vibration modes:  $\{1,2\}$ ,  $\{1,2,3\}$  and  $\{1,2,3,4\}$ .

## 5. RESULTS AND DISCUSSION

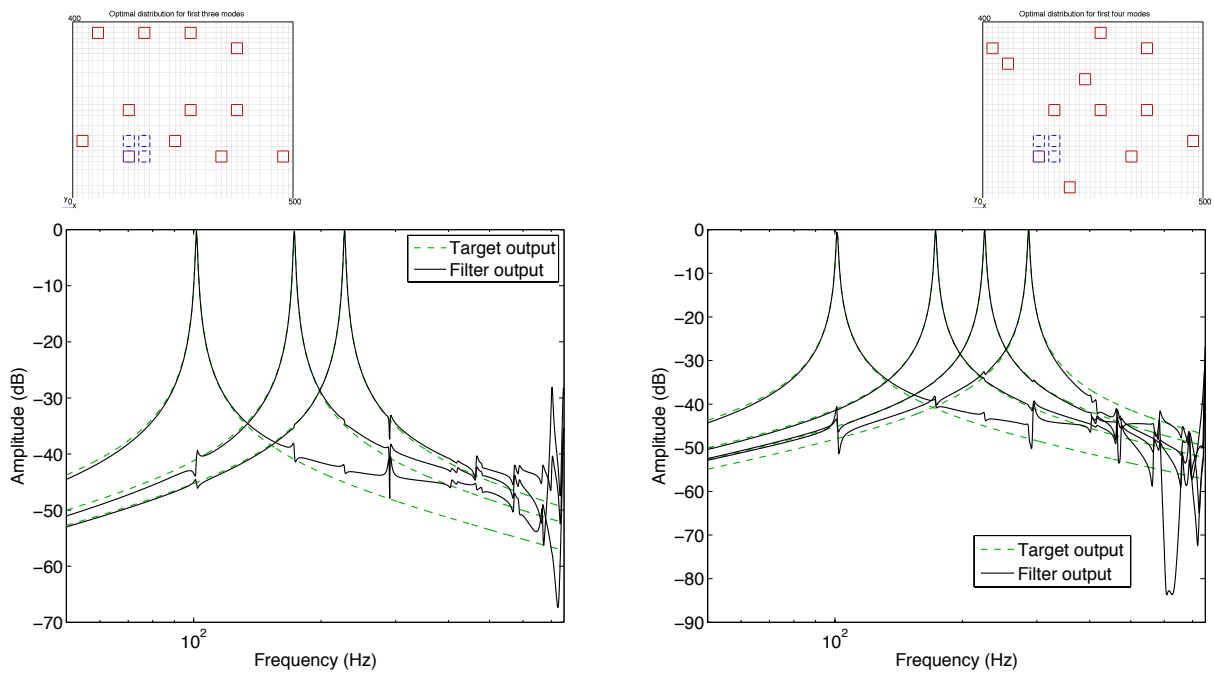
In this section, the results obtained for the modal filters with optimal topologies of arrays of sensors are presented. Based on previous studies, the following parameters were set for the GA optimization: initial population of 240 individuals, crossover rate at 40%, genic mutation rate at 4.6%, elite rate at 5% and termination criteria at 20 generations. The following figures present, for each one of the eight cases studied, the normalized filter output, such that the amplitude at target resonances is unitary, and the corresponding optimal distribution, in which the selected location for the twelve sensors are highlighted from the original array of 154 possible locations.

Figure 5 shows that distribution optimization for the design of modal filters aimed at isolating the first and second vibration modes has provided excellent performance up to 750 Hz, with filtering errors below 1% and 2%, for the first and first two modes respectively. It is also possible to observe that the sensors' distribution is not straightforward.

Figure 6 shows the normalized filter output when the first three and four modes are considered in the optimal design of the modal filters. For these cases, filtering is effective up to the truncation frequency



**Figure 5.** Normalized outputs of the modal filters designed for the isolation of the first (left) and first two (right) vibration modes.



**Figure 6.** Normalized outputs of the modal filters designed for the isolation of the first three (left) and first four (right) vibration modes.

of 750 Hz only and the unfiltered noise increases as the number of target modes increases, such that for three and four target modes, the unfiltered noise is below 4%. This suggests that as the number of target modes increases, it is harder to find a distribution that allows effective filtering for frequencies above the limiting frequency  $\omega_l$  (600 Hz in the present case).

In the case where the target function is multimodal, the filtering performance was also satisfactory with filtering errors below 4%, as shown in Figures 7, 8 and 9. It is worthwhile to notice that a multimodal response can be obtained by summing the individual weighting coefficients vectors such that the

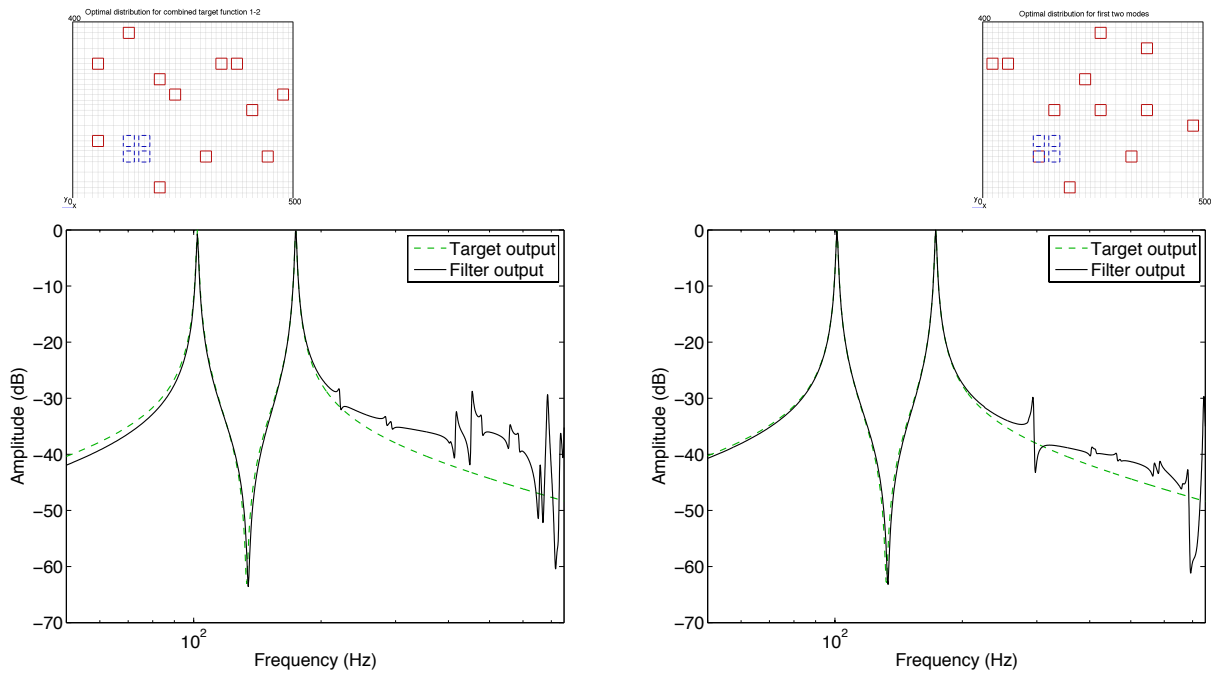


**Figure 7.** Normalized outputs of the modal filters designed for the simultaneous isolation of the first and second vibration modes, using two methodologies for the distribution optimization: (a) minimization of the error relative to a two-modes composed target function, (b) minimization of the mean errors relative to one-mode target functions.

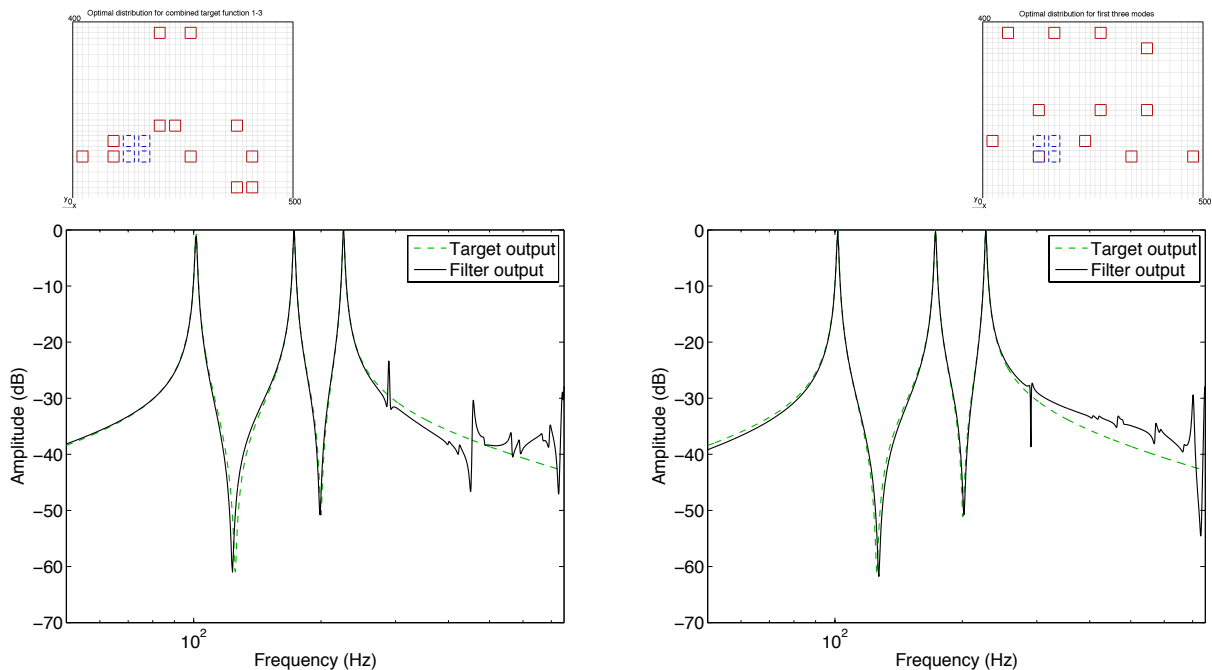


**Figure 8.** Normalized outputs of the modal filters designed for the simultaneous isolation of the first three vibration modes, using two methodologies for the distribution optimization: (a) minimization of the error relative to a three-modes composed target function, (b) minimization of the mean errors relative to one-mode target functions.

filter output simulates a multimodal target function by summing the approximation for the one-mode frequency responses. This is also shown in Figures 7, 8 and 9 where one may observe that both approaches lead to similar filtering performance although the sensors' distribution is quite different. Therefore, these

results indicate that it is more interesting to use the individual one-mode target functions for the distribution optimization, since the resulting distribution may be effective for the isolation of the target modes both individually and simultaneously.

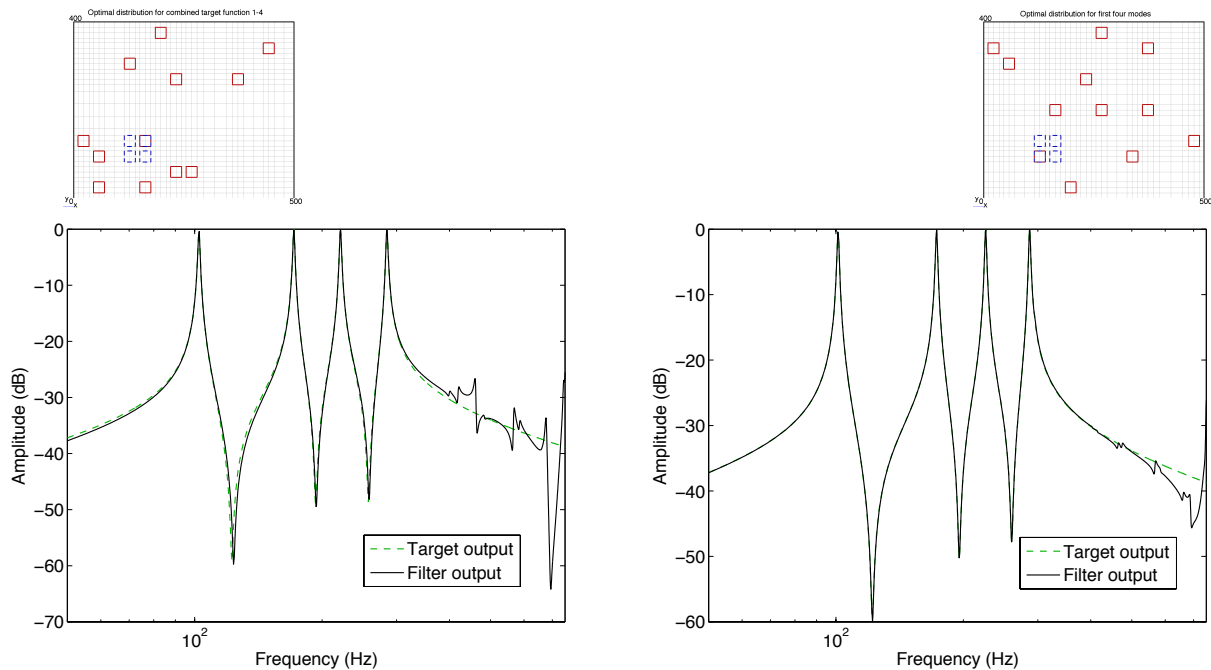


**Figure 9.** Normalized outputs of the modal filters designed for the simultaneous isolation of the first four vibration modes, using two methodologies for the distribution optimization: (a) minimization of the error relative to a four-modes composed target function, (b) minimization of the mean errors relative to one-mode target functions.

## 6. CONCLUSIONS AND FUTURE WORKS

This work presented a methodology for the optimization of the spatial distribution of a network of piezoelectric sensors with the objective of improving the performance of a set of modal filters. Genetic algorithm optimization techniques were used for the selection of 12 sensors, from an array of 154 piezoceramic sensors regularly distributed on an aluminum plate, which maximize the performance of a set of modal filters, each one aiming at one of the first four vibration modes. The weighting coefficients, for each modal filter, were evaluated using a QR decomposition of the complex frequency response function (FRF) matrix. Results have shown that the FRF inversion technique may provide high-performance modal filters for frequencies up to 600 Hz in this case. It is also shown that the sensors' distribution optimization may yield effective filtering of resonances beyond 600 Hz and up to 750 Hz, with filtering error depending on how many modal filters are considered in the design. Future works will be directed to experimental validation and application of the proposed modal filters for active vibration control.

## ACKNOWLEDGEMENTS

Support of MCT/CNPq/FAPEMIG National Institute of Science and Technology on Smart Structures in Engineering, grant 574001/2008-5, and FAPESP, grant 2014/16713-9, is acknowledged.

## REFERENCES

- [1] Sunar, M. and Rao, S.S., 1999, "Recent advances in sensing and control of flexible structures via piezoelectric materials technology," *Applied Mechanics Review*, 52(1), 1–16.
- [2] Chen, C.-Q. and Shen, Y.-P., 1997, "Optimal control of active structures with piezoelectric modal sensors and actuators," *Smart Materials and Structures*, 6(4), 403–409.
- [3] Sun, D., Tong, L. and Wang, D., 2001, "Vibration control of plates using discretely distributed piezoelectric quasi-modal actuators/sensors," *AIAA Journal*, 39(9), 1766–1772.
- [4] Tanaka, N. and Sanada, T., 2007, "Modal control of a rectangular plate using smart sensors and smart actuators," *Smart Materials and Structures*, 16(1), 36–46.
- [5] Fripp, M.L. and Atalla, M.J., 2001, "Review of modal sensing and actuation techniques," *The Shock and Vibration Digest*, 33(1), 3–14.
- [6] Preumont, A., François, A., De Man, P. and Piefort, V., 2003, "Spatial filters in structural control," *Journal of Sound and Vibration*, 265(1), 61–79.
- [7] Friswell, M., 2001, "On the design of modal actuators and sensors," *Journal of Sound and Vibration*, 241(3), 361–372.
- [8] Lee, C.K. and Moon, F.C., 1990, "Modal sensors/actuators," *Journal of Applied Mechanics*, 57(2), 434–441.
- [9] Shelley, S.J., 1991, "Investigation of discrete modal filters for structural dynamic applications," PhD thesis, University of Cincinnati.
- [10] Deraemaeker, A. and Preumont, A., 2006, "Vibration based damage detection using large array sensors and spatial filters," *Mechanical System and Signal Processing*, 20(7), 1615–1630.
- [11] Staszewski, W.J., Worden, K., Wardle, R. and Tomlinson, G.R., 2000, "Fail-safe sensor distributions for impact detection in composite materials," *Smart Materials and Structures*, 9(3), 298–303.
- [12] Meirovitch, L. and Baruh, H., 1982, "Control of self-adjoint distributed-parameter systems," *AIAA Journal of Guidance, Control and Dynamics*, 5(1), 60–66.
- [13] Leo, D.J. and How, J.P., 1997, "Reconfigurable actuator-sensor arrays for the active control of sound," *Proceedings of SPIE Smart Structures and Materials: Smart Structures and Integrated Systems*, Vol. 3041, San Diego, CA.
- [14] Baz, A. and Poh, S., 1990, "Experimental implementation of the modified independent modal space control method," *Journal of Sound and Vibration*, 139(1), 133–149.
- [15] Begg, D.W. and Liu, X., 2000, "On simultaneous optimization of smart structures - part ii: algorithms and examples," *Computer Methods in Applied Mechanics and Engineering*, 184(1), 25–37.
- [16] Frecker, M.I., 2003, "Recent advances in optimization of smart structures and actuators," *Journal of Intelligent Material Systems and Structures*, 14(4-5), 207–216.
- [17] Kogel, M. and Silva, E.C.N., 2005, "Topology optimization of smart structures: design of piezoelectric plate and shell actuators," *Smart Materials and Structures*, 14(2), 387–399.
- [18] Goldberg, D., 1989, "Genetic algorithms in search, optimization, and machine learning," Addison-Wesley Pub. Co..
- [19] Pagani Jr., C.C. and Trindade, M.A., 2009, "Optimization of modal filters based on arrays of piezoelectric sensors," *Smart Materials and Structures*, 18(9), art.no.095046.
- [20] Trindade, M.A., Pagani Jr., C.C. and Oliveira, L.P.R., 2011, "Semi-modal active vibration control of plates using discrete piezoelectric modal filters," In *22nd International Conference on Adaptive Structures and Technologies (ICAST'2011)*, Corfu.
- [21] Trindade, M.A., Pagani Jr., C.C., Oliveira, L.P.R. and Massaroppi Jr., E., 2013, "Effect of parametric uncertainties on the effectiveness of discrete piezoelectric spatial modal filters," *International Journal for Uncertainty Quantifications*, 3, 523-540.